Clim Dyn
DOI 10.1007/s00382-012-1427-8

A new paradigm for the predominance of standing Central Pacific Warming after the late 1990s

Baoqiang Xiang · Bin Wang · Tim Li

Received: 29 March 2012 / Accepted: 14 June 2012

Abstract Canonical El Niño has a warming center in the eastern Pacific (EP), but in recent decades, El Niño warming center tends to occur more frequently in the central Pacific (CP). The definitions and names of this new type of El Niño, however, have been notoriously diverse, which makes it difficult to understand why the warming center shifts. Here, we show that the new type of El Niño events is characterized by: 1) the maximum warming standing and persisting in the CP and 2) the warming extending to the EP only briefly during its peak phase. For this reason, we refer to it as standing CP warming (CPW). Global warming has been blamed for the westward shift of maximum warming as well as more frequent occurrence of CPW. However, we find that since the late 1990s the standing CPW becomes a dominant mode in the Pacific; meanwhile, the epochal mean trade winds have strengthened and the equatorial thermocline slope has increased, contrary to the global warming-induced weakening trades and flattening thermocline. We propose that the recent predominance of standing CPW arises from a dramatic decadal change characterized by a grand La Niña-like background pattern and strong divergence in the CP atmospheric boundary layer. After the late 1990s, the anomalous mean CP wind divergence tends to weaken the anomalous convection and shift it westward from the underlying SST warming due to the *suppressed low-level convergence feedback*. This leads to a westward shift of anomalous westerly response and thus a zonally in-phase SST tendency, preventing eastward propagation of the SST anomaly. We anticipate more CPW events will occur in the coming decade provided the grand La Niña-like background state persists.

Keywords Central Pacific Warming · La Niña-like mean state change · Convection · Low-level convergence feedback

B. Xiang (✉) · B. Wang · T. Li
International Pacific Research Center, School of Ocean and Earth Science and Technology, University of Hawaii, 1680 East–West Rd., Honolulu, HI 96822, USA
e-mail: baoqiang@hawaii.edu

B. Wang · T. Li
Department of Meteorology, School of Ocean and Earth Science and Technology, University of Hawaii, 2525 Correa Rd., Honolulu, HI 96822, USA

1 Introduction

El Niño/Southern Oscillation (ENSO) exerts far-reaching effects on global climate. Investigation of ENSO property change is of utmost importance to strategic planning of agriculture, water supplies and ecosystems. In contrast to the canonical El Niño in the eastern Pacific (EP Warming, or EPW for short), recent studies found a new type of El Niño with its maximum warming in the equatorial central Pacific (CP) (Larkin and Harrison 2005; Ashok et al. 2007; Kao and Yu 2009; Kug et al. 2009; Yeh et al. 2009). In addition, the amplitude of this new type of El Niño has increased in recent decades (Lee and McPhaden 2010). For convenience, hereinafter we refer this new type of El Niño as to CP warming (CPW).

Compared with the canonical EPW, the CPW exhibits distinctly different impacts on worldwide climate. For example, the CPW shifts the anomalous convection westward and usually forms two anomalous Walker circulations in the tropical Pacific (Ashok et al. 2007; Weng et al. 2007; Weng et al. 2009). The westward displaced convection was suggested to be more effective in causing Indian drought

Published online: 15 July 2012

(Kumar et al. 2006). The CPW increases hurricane frequency both in the Atlantic Ocean (Kim et al. 2009) and western North Pacific (Chen and Tam 2010), and also shifts tropical cyclone tracks in the western North Pacific (Hong et al. 2011). The CPW is tightly linked to a decadal variation of the North Pacific Gyre Oscillation and the marine ecosystems (Di Lorenzo et al. 2010). In recent decades, the warming trend in the CP can also cause the west Antarctic warming associated with the atmospheric Rossby waves propagation (Ding et al. 2011). Therefore, exploring the cause of this observed warming center shift is of great importance to climate prediction and understanding future changes in ENSO.

The fundamental cause of the more frequent and intensified CPW in recent decades remains a matter of debate. A recent study argued that the more frequent occurrence of CPW could be a consequence of global warming (Yeh et al. 2009). With anthropogenic forcing, the Walker circulation and the associated trade winds tend to be weakened so that the equatorial thermocline becomes shoaled and flattened, serving to enhance the thermocline feedback in the CP as well as more frequent occurrence of CPW (Yeh et al. 2009). This explanation may be working in the future warming environment, but does not seem to explain what has happened in the past three decades. McPhaden et al. (2011) pointed out that the background mean state change in recent decades is opposite to that expected from anthropogenic forcing, the former characterized by enhanced trade winds and more tilted thermocline. Meanwhile, global warming has leveled off after the late 1990s (e.g., Solomon et al. 2010), whereas the CPW has been increasing its frequency and intensity.

In this study, we offer a new mechanism by spotlighting the importance of the mean state change in Pacific basin characterized by a La Niña-like pattern. This paper is organized as follows. Data, methodology and models are introduced in Sect. 2. Section 3 investigates the observational El Niño property change after the late 1990s and the contrasting features between the EPW and CPW. In Sect. 4, we examine how the annual mean modulates the anomalous convection as well as the El Niño behaviors. Finally, in Sect. 5 we summarize the major findings in this study and discuss the possible factors inducing this mean state change.

2 Data, methodology and models

We use several monthly mean datasets, including wind data from NCEP-DOE (National Centers for Environmental Prediction–Department of Energy) AMIP-II Reanalysis products (Kanamitsu et al. 2002), precipitation from GPCP (Global Precipitation Climatology Project, v2.2) (Adler et al. 2003), and SST from ERSST (NOAA Extended Reconstructed SST, v3b) (Smith et al. 2008). We also use an ocean reanalysis dataset GODAS (Global Ocean Data Assimilation System) (Behringer and Xue 2004), forced with NCEP-DEO AMIP-II surface wind stress. Due to data availability, the study period is between 1980 and 2010. To the first-order approximation, we interpret a rising sea surface height (SSH) as a deepened thermocline. In this paper, we separate the studied period into two epochs, i.e., 1980–1998 and 1999–2010, and the anomalous fields are calculated by subtracting the corresponding climatology in each epoch to avoid the contamination of decadal change signals. This is mainly due to the large mean state change in the two epochs.

Two atmospheric models are used in this study. The first is the atmospheric model component of the Zebiak-Cane (ZC) coupled model (Zebiak and Cane 1987). In this model, the atmospheric deep convective heating is associated with two different processes, the climatological and anomalous SST related heating ($\mathbf{Q_s}$) and the low-level convergence related heating ($\mathbf{Q_1}$)

$$Q_s = (\alpha T)\exp\left[\frac{\overline{T} - 30\,^{\circ}\mathrm{C}}{16.7\,^{\circ}\mathrm{C}}\right] \quad (1)$$

$$Q_1 = \beta\,[M(\bar{c} + c) - M(\bar{c})] \quad (2)$$

where

$$M\ (x) = \begin{cases} 0, X \le 0 \\ X, X > 0 \end{cases} \quad (3)$$

where $\overline{T}$, T are the climatological SST and SST anomaly (SSTA), respectively. $\bar{c}$, c are the climatological and anomalous low-level convergence. α and β are coefficients associated with these two different heatings. The implication for Q_1 is that the low-level convergence feedback can generate deep heating only when the sum of the climatological and anomalous low-level winds is convergent. More detailed can be found in Zebiak and Cane (1987).

The other atmospheric model we used is the ECHAM (v4.6) model (Roeckner et al. 1996). Five experiments (three control and two sensitivity experiments) are performed and each has 12 ensembles (Table 1). The first one (CTRL_ID1_old) uses the climatological SST forcing in the first epoch (1980–1998). The second one (CTRL_ID1) is the same as CTRL_ID1_old but with imposed low-level (approximately from 850 to 1000 hPa) wind convergence. The third one (CTRL_ID2) uses the climatological SST forcing in the second epoch (1999–2010). Based on the last two control runs (CTRL_ID1 and CTRL_ID2), we make two sensitivity experiments with prescribed SST warming in the CP (SEN_ID1 and SEN_ID2) to examine the different atmospheric responses particularly for the anomalous precipitation and surface wind (Table 1).

Table 1 List of three control experiments and two sensitivity experiments by using the ECHAM atmospheric model

Experiments	Description
CTRL_ID1_old	Forced by climatological SST in the first epoch 1980–1998 which shows an unrealistic strong low-level wind divergence pattern compared with observations (Fig. 10a vs. Fig. 8a)
CTRL_ID1	Forced by climatological SST in the first epoch 1980–1998 but with imposed low-level wind convergence (Fig. 10d) to obtain a more realistic mean low-level wind convergence pattern
CTRL_ID2	Forced by climatological SST in the second epoch 1999–2010
SEN_ID1	The same as CTRL_ID1 together with anomalous SST forcing in the CP as shown in Fig. 11a
SEN_ID2	The same as CTRL_ID2 together with anomalous SST forcing in the CP as shown in Fig. 11a

3 Observed change of El Niño property after the late 1990s

A major problem about the new type of El Niño is that the phenomenon has been described with enormous diversity, which makes it difficult to study the mechanism leading to the observed ENSO property change. Different terminologies have been used to describe this new type of El Niño, such as 'Dateline' El Niño (Larkin and Harrison 2005), El Niño Modoki (Ashok et al. 2007), CP El Niño (Yeh et al. 2009; Kao and Yu 2009), Warm Pool El Niño (Kug et al. 2009), and CPW (Kim et al. 2009). Meanwhile, the definitions of the new type of El Niño differ widely from each other in previous studies. As a result, a total of 10 cases of new type of El Niño have been identified in the past three decades (Table 2). Among the 10 cases there are only 4 robust cases (1994, 2002, 2004, 2009) that are consistently categorized as CPW for all these studies (Table 2), and the other six are disputable cases (1986, 1987, 1990, 1991, 1992, 2001).

Actually these four robust CPW cases exhibit close similarity in their evolution patterns and phase locking (Fig. 1). In contrast, the disputable cases have very different features. For instance, several cases are not phase-locked in boreal winter (1986, 1987, 1990, 1992, 2001); Case 1991 has maximum warming in the CP during boreal winter but the maximum SST warming is located in the EP during its developing summer and decaying spring (Fig. 1). We will discuss more about the characteristics of CPW differing from EPW in Sect. 3.1.

Since three out of four robust CPW occur after the late 1990s, one would wonder whether the behavior of the leading mode of SSTA has changed. Figure 2 shows that the first leading empirical orthogonal function (EOF) mode of the tropical Pacific SSTA has indeed changed after the late 1990s with its maximum center shifting to the CP (around 150°W). It largely reflects the fact that, during the latter epoch, three out of four cases are robust CPW cases except one weak EPW event (2006). It is interesting to note that the CPW in this study is different from the El Niño Modoki (Ashok et al. 2007) to some extent since the EOF-2 mode does not change much during these two epochs (not shown). Based on the EOF-2 mode, El Niño Modoki emphasizes the SSTA gradient in the tropical Pacific which exhibits an out-of-phase between the CP, and the WP and EP (Ashok et al. 2007). However, some other studies proposed some criteria to define this new type of El Niño by comparing the relative intensity of SSTA in the CP and EP during boreal winter (Yeh et al. 2009; Kug et al. 2009; Kim et al. 2009; McPhaden et al. 2011). The El Niñoo Modoki is not phased locked to boreal winter (Ashok et al. 2007), and seems to be a more broader definition which includes more cases than others (Table 2).

3.1 Evolution and structure differences between EPW and CPW

Before discussing the causes of the El Niño property change, we need to first identify the major differences between EPW and robust CPW by comparing their time evolution patterns. Based on the fact that the EPW (CPW) dominates over the first (second) epoch and the majority of the robust CPW occur in the second epoch, we use the two strong cases of 1982, 1997 as EPW and 2002, 2004, 2009 as robust CPW to make the composite analysis (Fig. 3). Due to the relatively less events and short period of these two epochs, one may wonder whether this epochal contrast is meaningful. We will discuss this in Sect. 4.3.

For the EPW, deepened thermocline emerges in the equatorial western Pacific (WP) as a precursor of the El Niño, which then proceeds eastward steadily (Fig. 3b). Once the thermocline anomaly reaches the CP, it

Table 2 Cases of this new type of El Niño for different definitions

El Niño Modoki (Ashok et al. 2007)	Warm Pool El Niño (Kug et al. 2009)	CP-El Niño (Yeh et al. 2009)	CP Warming (Kim et al. 2009)	CP-El Niño (McPhaden et al. 2011)
86, 90, 91, 92, 94, 02, 04, 09	90, 94, 02, 04, 09	90, 94, 01, 02, 04, 09	91, 94, 02, 04, 09	87, 94, 02, 04, 09

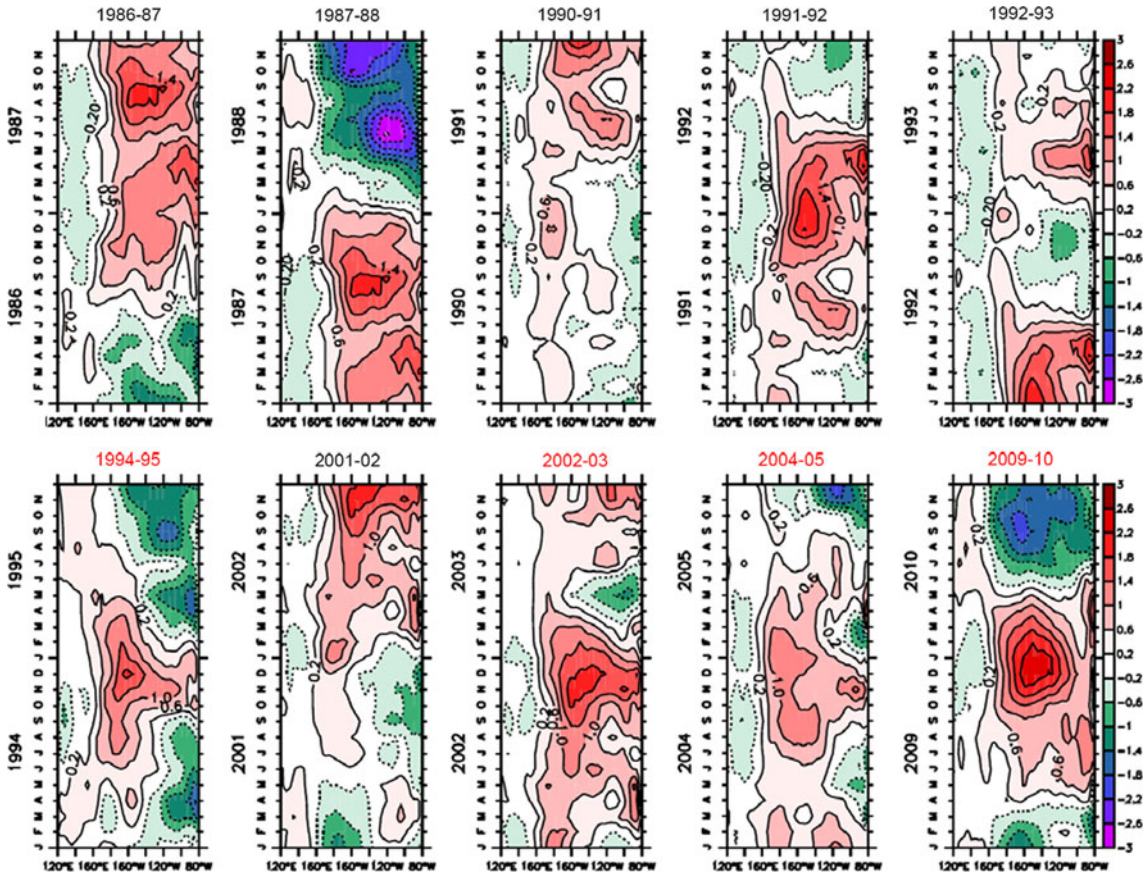

Fig. 1 Longitude-time *diagram* of the equatorial (2°S–2°N) SSTA for 10 cases that are selected as CPW from previous studies (Table 2). The years with *red marks* denote the robust CPW cases

propagates eastward rapidly, ending up with a prominent warming in the equatorial eastern EP. Through Bjerknes feedback (Bjerknes 1969), the EP SST warming reinforces anomalous convection and surface westerly anomalies to the west, so that the convection and westerly anomalies migrate eastward accordingly and further feed back to the EP SST warming (Fig. 3a, b). After boreal winter, the EP SST warming sustains for a longer period than the CP SST warming. But this primarily owes to its strong peak amplitude instead of a weak damping rate in the EP. Actually the EP SST warming decays earlier and more significantly than the CP SST warming (Fig. 4a).

By contrast, for the robust CPW, initiation of the deepening thermocline and SST warming occurs in the region near the dateline (160°E–160°W) (Fig. 3d). Interestingly, the corresponding anomalous surface zonal wind stress is very weak during the onset stage. Although the maximum warming and the deepest thermocline anomaly areas expand toward the EP slowly, both of their maxima never reach the EP, indicating a standing feature. In accord with the quasi-stationary oceanic anomalies, the enhanced convection and westerly anomalies are trapped in the region west of 160°W without clear eastward propagations (Fig. 3c). Compared with the EPW, this relatively westward shifted anomalous convection and zonal wind stress anomaly (about 20° of longitude) are also apparent for the regression pattern with respect to the first leading mode during two epochs (Fig. 2c, d). This comparison between EPW and CPW is generally consistent with other studies (Ashok et al. 2007; Kao and Yu 2009; Yu et al. 2010) and coupled model results (Choi et al. 2011). After boreal winter, the weak EP SST warming decays abruptly while the CP SST warming persists until the next summer (Fig. 3d). That is, the EP warms up slowly but decays rapidly, resulting in an aborted warming in the EP. A strengthening of easterly anomalies is observed in the EP from March of the developing year to May of the decay year for CPW, while no clear wind anomalies in the EP during the developing phase but northeasterly anomalies prevail in the decay phase for EPW (Fig. 4). Given the wind pattern difference, it is plausible to infer that the processes determining the rapid decay of the EP SST warming are different. The rapid decay of EP SST warming for CPW is likely related to enhanced latent heat flux, anomalous zonal advection and vertical entrainment, while

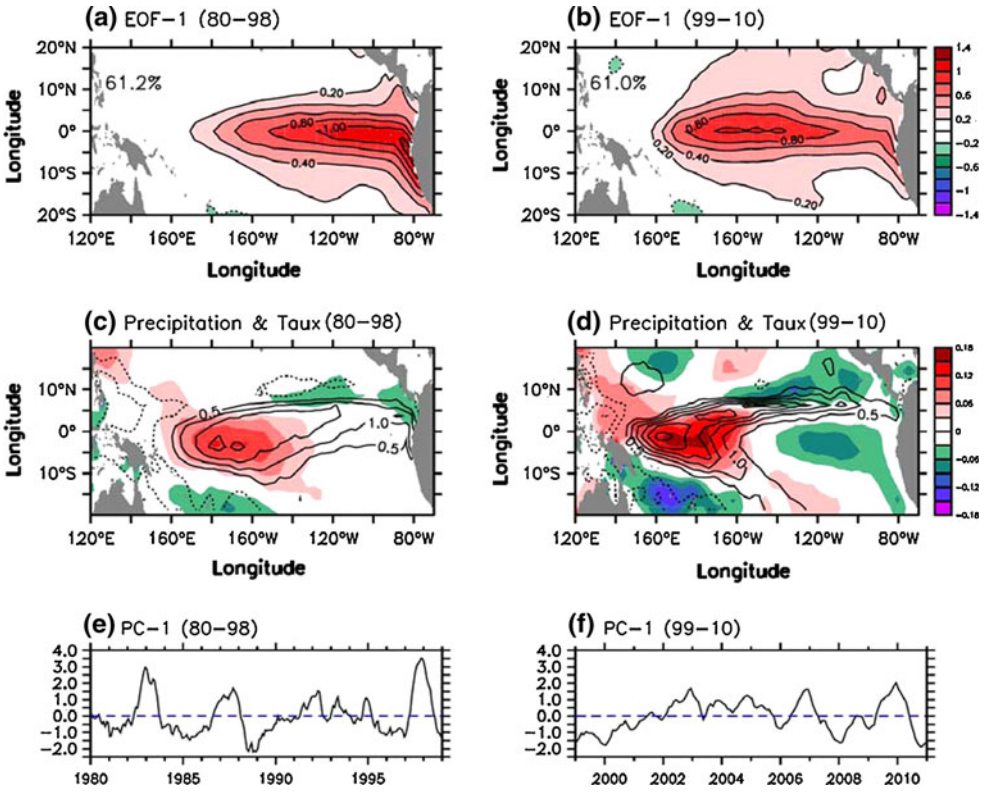

Fig. 2 The leading EOF mode of monthly mean SSTA in the tropical Pacific domain during **a** 1980–1998 and **b** 1999–2010. The fractional variance that can be explained by the EOF-1 mode is 61.2 %, 61.0 %, respectively. **c** and **d** Linear regression of precipitation anomaly (contours in mm/day) and surface zonal wind stress anomaly (*shading* in dyn/cm^2) onto the time series of EOF-1 mode during these two epochs as shown in **e** and **f**, respectively

the decay of EPW is mainly due to less solar radiation resulting from enhanced precipitation (Fig. 3a).

Examination of the equatorial SSTA tendency also helps gain insight into the dynamics governing the different evolution between EPW and CPW (Fig. 4). Two common features for EPW and CPW are: (1) Strong SSTA tendency occurs in both boreal spring and fall and it is relatively weak in boreal summer; (2) The positive SSTA tendency tends to initiate and develop from the CP, but the SST warming prefers to decay from the EP to the CP. More importantly, two strikingly different features are summarized as, (1) the SST warming tendency for CPW is much weaker than EPW during its onset/developing stages together with weaker surface westerly anomalies; (2) in boreal spring, the maximum SSTA tendency of the EPW proceeds eastward and becomes most pronounced in the EP, however, the positive SSTA tendency of the CPW only exhibits a weak eastward extension. It accounts for the fact that the EP SST warming has a relatively shorter developing period, weaker amplitude and less persistence for CPW.

Boreal spring is one of the key seasons with rapid intensification of El Niño together with distinct zonal contrast of SSTA tendency between EPW and CPW (Fig. 4). In the next section, we will focus on April–May, during which both the SST warming anomalies for CPW and EPW are residing in the CP (Fig. 5), providing an opportunity to examine the dynamics leading to the different evolutions in the following months.

3.2 Contrast of CPW and EPW development in boreal spring

The different behaviors of El Niño development during boreal spring have profound impacts on the further development. As seen in Fig. 3b and d, after boreal spring SSTA associated with CPW continues growing over the CP while SSTA associated with EPW moves eastward. This implies that the SSTA tendency is very different between CPW and EPW at that time. It is seen from Fig. 4 that in April–May the maximum SSTA tendency for EPW is located over EP while it is primarily located in CP for CPW. What causes such a tendency contrast while the warm SSTA for both cases appears in the CP? Here we compare the spatial patterns of these two types of El Niño in April–May (Fig. 5). Clearly, the EPW-related precipitation and wind anomalies are zonally in-phase with the underlying SSTA, whereas the CPW-related precipitation and zonal zonal wind anomalies shift to the west of the maximum SSTA center (Fig. 5a, c). As a result, the CPW-related zonal wind stress anomaly exhibits a rather zonal symmetric structure with westerly anomalies in the WP and easterly anomalies in the EP (Fig. 5c), so that the maximum thermocline anomaly is

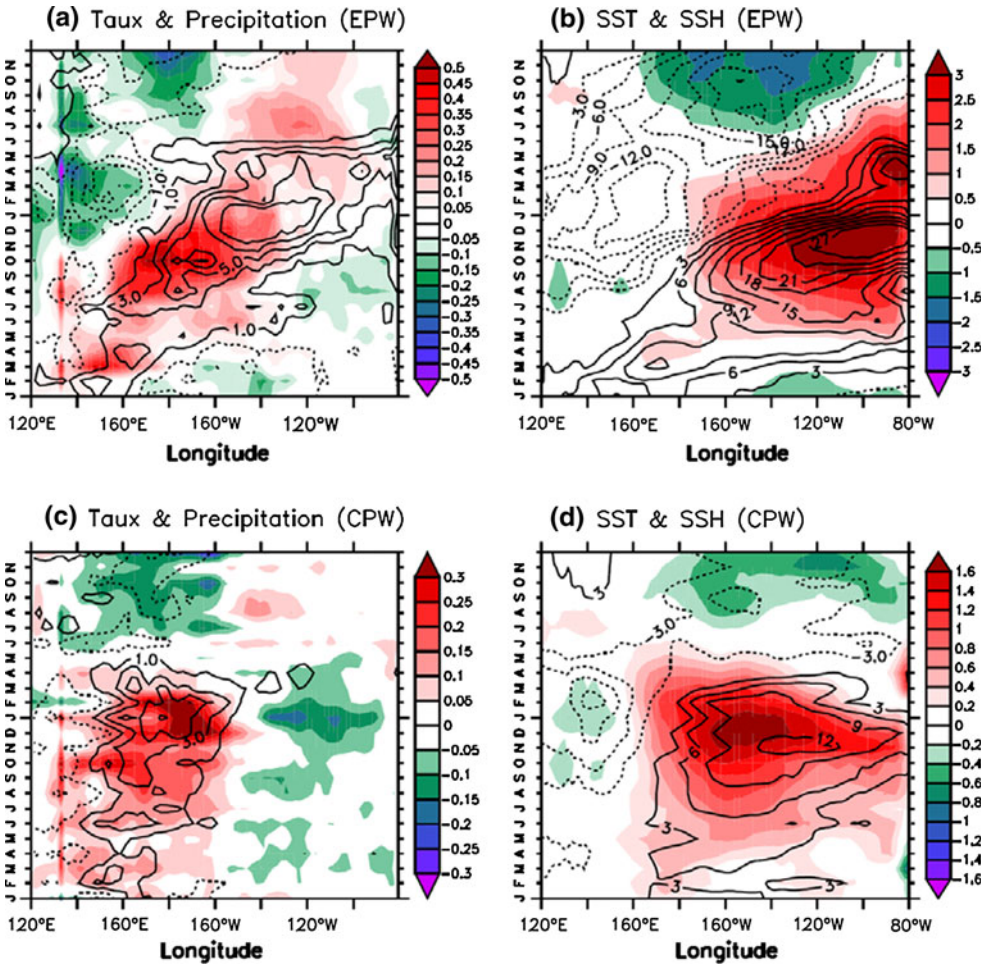

Fig. 3 Evolution of the composite EPW (1982, 1997, *upper panel*), and CPW (2002, 2004, 2009, *lower panel*) averaged between 2°S and 2°N. **a** and **c** show the anomalous zonal wind stress (*shaded* in dyn/cm^2) and precipitation (contours in mm/day). **b** and **d** display the SSTA (*shaded* in °C) and SSH anomaly (contours in cm). Note that zonal wind stress anomaly and SSTA use *different color* scale for EPW and CPW

confined in the CP (Fig. 5d). This is in contrast with the EPW case in which the zonally in-phase wind stress anomaly leads to a maximum response of thermocline depth anomaly in the EP (Fig. 5c). It is anticipated that such distinctive thermocline depth anomaly responses would result in distinctive SSTA tendency between the two types of El Niño.

Li (1997) and Jin et al. (2006) suggested that three feedbacks are mainly responsible for the ENSO development, namely, the thermocline (TH) feedback (mean vertical advection of anomalous vertical temperature gradient), zonal advection (ZA) feedback (anomalous zonal advection of mean zonal SST gradient) and Ekman pumping (EK) feedback (anomalous vertical advection of mean vertical SST gradient). The TH, ZA, EK feedbacks can be expressed as $-\overline{w}\frac{DT_e}{Dz}$, $-u\frac{D\overline{T}}{Dx}$, and $-w\frac{D\overline{T}}{Dz}$, where $\overline{w}$, u and w represent the equatorial mean upwelling, anomalous zonal current and vertical upwelling, respectively. T_e and $\overline{T}$ denote the subsurface temperature anomaly and climatological upper ocean temperature, respectively. The deepened thermocline can also drive an upper-ocean eastward current as a geostrophic component (Su et al. 2010), facilitating an eastward advection as well as a positive ZA feedback. Meanwhile, the strong zonal current can also induce a downwelling anomaly in the EP, which in turn intensifies the local EK feedback.

Examination of the GODAS reanalysis data sets offers evidence in explaining the contrasting SSTA tendency between the EPW and CPW (Fig. 6). For the EPW, both the TH feedback and the EK feedback are stronger in the EP (120°W–80°W, 2°S–2°N) than the CP (170°W–130°W, 2°S–2°N) (Fig. 6a). Therefore, the occurrence of maximum temperature tendency in the EP favors the eastward migration of the coupled system in the EPW case. For the CPW, however, all the three feedbacks are negative (positive) in the EP (CP) (Fig. 6b). This explains why the CPW exhibits a nearly standing feature (with no clear eastward propagation). The difference of the three feedbacks between the EPW and CPW is primarily attributed to distinctive surface wind-SST zonal phase relationships as illustrated in Fig. 5a, c.

Near the equator, the zonal gradient of thermocline anomaly is approximately in Sverdrup balance with zonal wind stress anomaly (Li 1997). Thus, the magnitude and

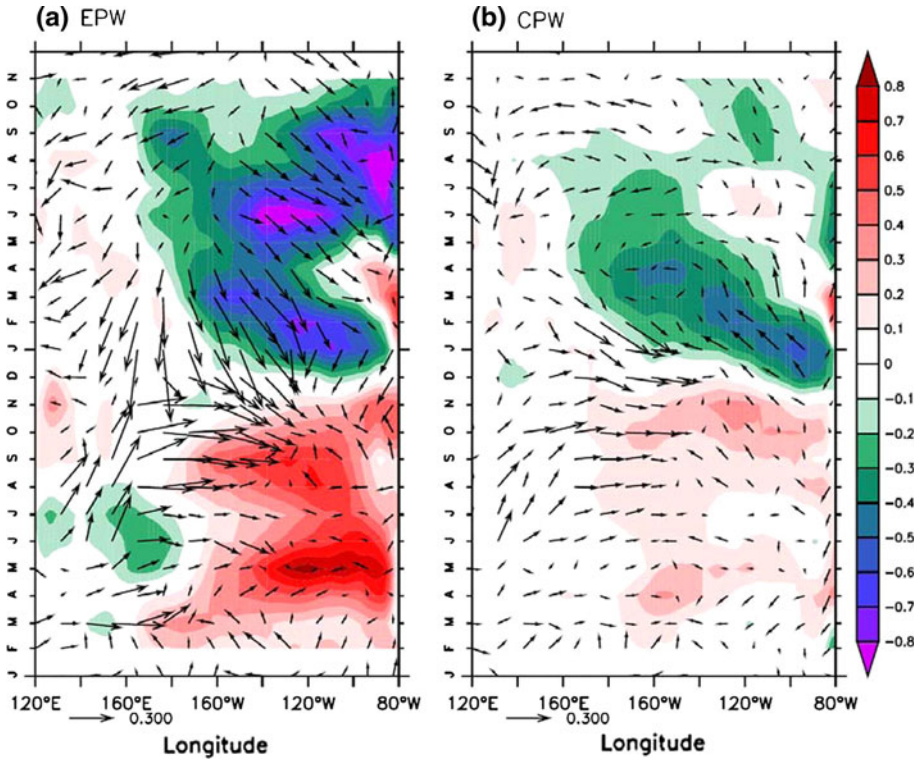

Fig. 4 Equatorial (2°S–2°N) SSTA tendency (*shading* in °C/month) and wind stress anomaly (vectors in dyn/cm^2, 5°S–5°N) for the composite **a** EPW and **b** CPW

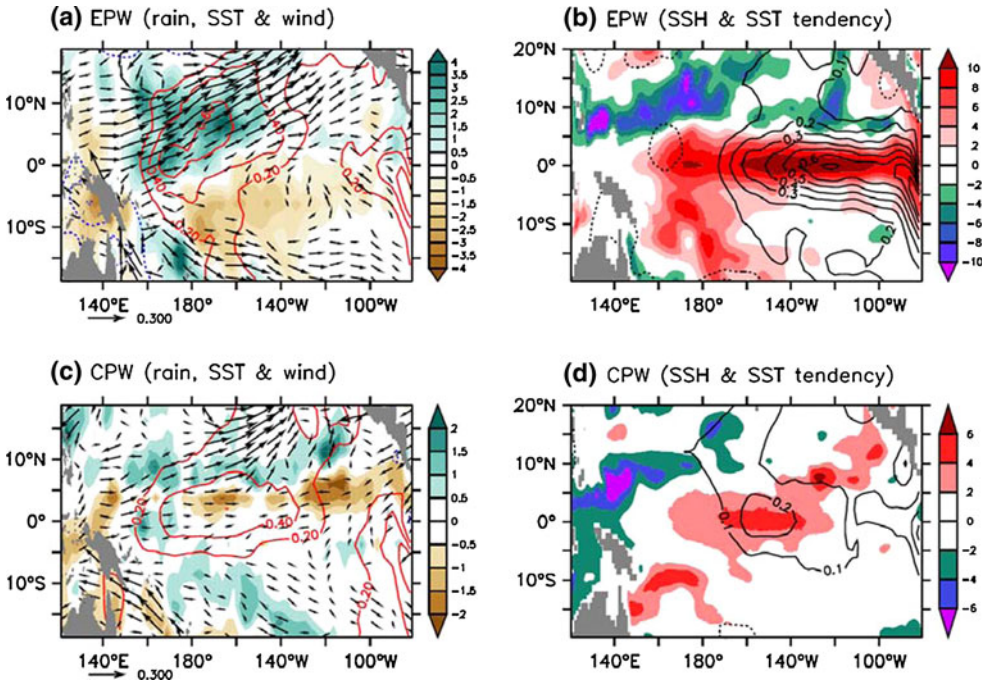

Fig. 5 Contrast of the spatial pattern of composite SSTA (contours in °C), wind stress (vectors shown only when its absolute value greater than 0.05 dyn/cm^2) and precipitation anomaly (*shading* in mm/day) during the onset stage (April–May) for **a** EPW **c** CPW. The *right panels* **b** and **d** are the corresponding SSH anomaly (*shading* in cm) and SSTA tendency (contour in °C/month)

location of the thermocline depth anomaly rely greatly on the zonal surface wind anomaly, and the maximum thermocline anomaly mostly appears in the region where the surface wind changes from westerly to easterly anomalies. This is indeed the case as one can see from Fig. 3 that the positive surface wind anomalies are always located to the west of maximum thermocline depth anomalies. Therefore, revealing what causes the distinctive SST-precipitation-zonal wind phase relations during the period when both the SST warming anomalies are located in the CP holds a key for understanding the physical mechanisms of the formation of CPW and EPW.

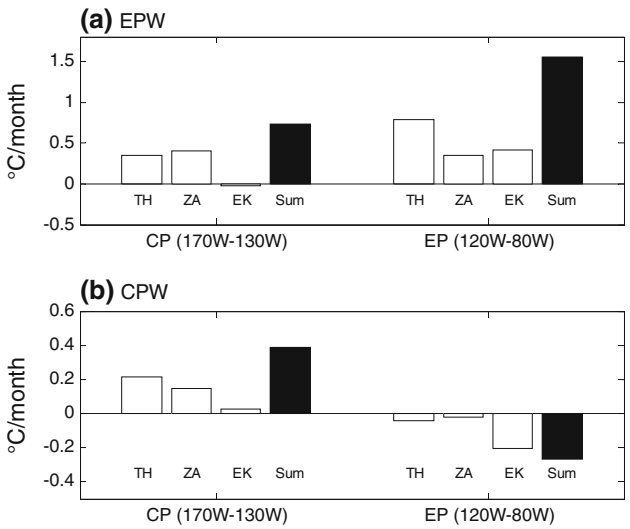

Fig. 6 A composite budget analysis of the contributions of various processes to the mixed layer temperature tendency averaged over the CP (170°W–130°W, 2°S–2°N) and EP (120°W–80°W, 2°S–2°N) for **a** EPW and **b** CPW during April–May. The *open white bars* in each *panel* represent the thermocline (TH) feedback, zonal advection (ZA) feedback and Ekman pumping (EK) feedback, respectively. The *closed black bars* denote the sum of the above three terms. The mixed layer depth used here is 40 m for CP and 10 m for EP

4 A new paradigm for the dominance of standing CPW

Variation of the ocean–atmosphere mean state has profound impacts on ENSO behaviors (e.g., Wang 1995; Li and Hogan, 1999; Fedorov and Philander 2000; An and Wang 2000). Particularly, Choi et al. (2011) emphasized the role of the decadal mean state in modulating an El Niño's flavor, and found that CPW tends to occur more frequently when the zonal mean SST gradient is stronger over the tropical Pacific. Hence, investigation of mean state change may be instrumental in clarifying the basic mechanism for the predominance of the standing CPW since the late 1990s.

4.1 Observed decadal mean state change

Figure 7 portrays the mean state differences between these two epochs (1999–2010 minus 1980–1998). The SST change exhibits a La Niña-like pattern characterized by SST cooling in the equatorial CP and subtropical EP, and SST warming in other regions of the Pacific domain (Fig. 7a). The associated mean precipitation is substantially suppressed in the equatorial Pacific particularly near the dateline, and the mean precipitation is reduced by about 27 % in the CP (170°E–130°W, 5°S–5°N) (Fig. 7b). Consistently, enhanced trades and more strongly east–west tilted thermocline appear in the second epoch (Fig. 7c).

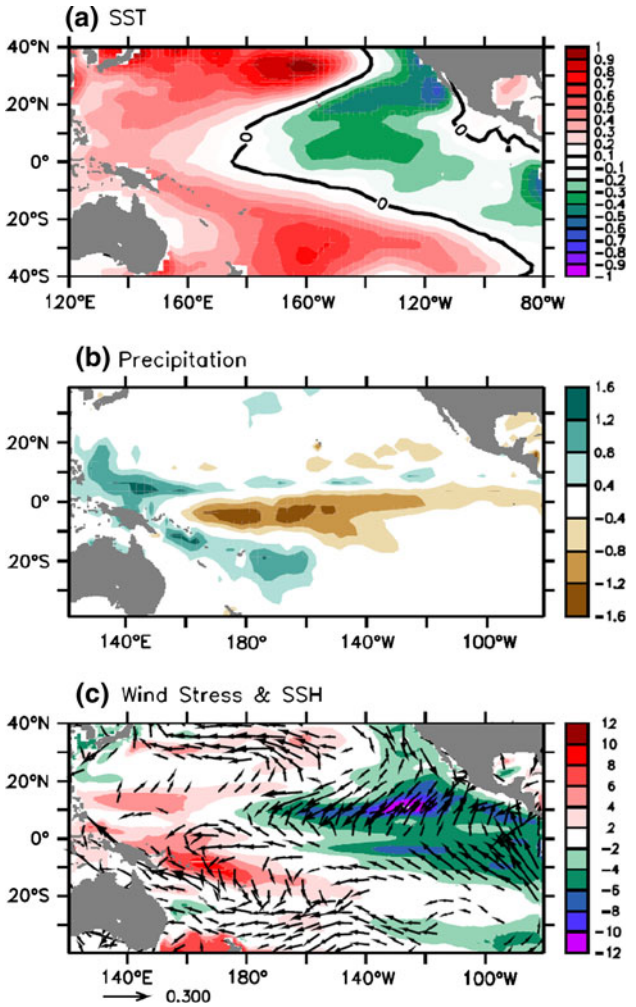

Fig. 7 Epochal differences (1999–2010 minus 1980–1998) of **a** SST (°C), **b** precipitation (mm/day), **c** SSH (*shading* in cm) and surface wind stress (vectors shown only when its absolute value greater than 0.05 dyn/cm^2)

Previous studies suggested that anomalous convection to a great degree depends on mean SST distribution and mean low level wind convergence (e.g., Zebiak 1986; Zebiak and Cane 1987). Mean SST cooling leads to less sensitivity of anomalous convection to SSTA (Eq. 1). This is well supported by investigating current climate models. The majority of current climate models have the problem of excessive cold tongue extension, and this equatorial cold SST bias displaces the anomalous convection toward the west (Ham and Kug 2011; Xiang et al. 2011). This resultant westward shift of convective anomaly severely limits the ability of coupled models in successfully simulating two types of El Niño (Ham and Kug 2011).

The deep convective heating is also strongly coupled to the low-level moisture convergence. The condensation-induced convective heating tends to result in lower surface pressure as well as more convergence, which then feeds

back to enhance the convective heating. This is similar to the CISK (conditional instability of the second kind) mechanism. Therefore, this La Niña-like SST change is also able to alter the anomalous convection via changing mean low-level convergence. According to the assumption in the ZC atmospheric model, the development of low-level convergence-related heating requires a convergence for the sum of the anomalous and climatological fields. As shown in Fig. 8, the mean low-level (1,000 hPa) convergence is approximately zero in the CP during the first period, while it becomes prominently divergent in the second epoch. We hypothesize that the mean low-level divergence together with subsidence may inhibit the development of anomalous deep convection over the region east of international dateline, causing the nearly stationary convection and low-level wind anomalies confined to the WP.

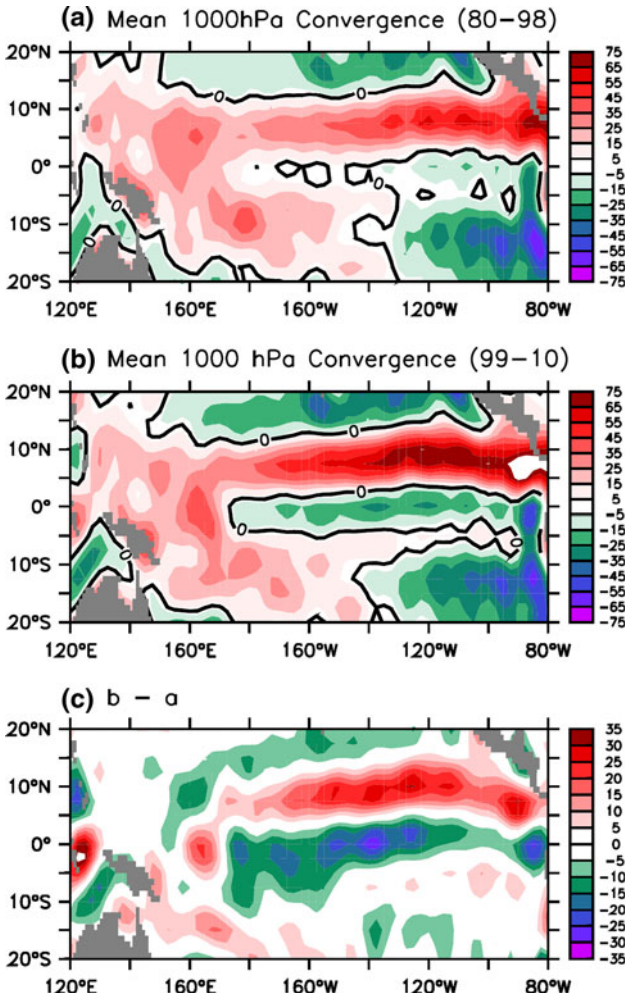

Fig. 8 Mean low-level (1,000 hPa) wind convergence ($\times 10^{-7}$ s^{-1}) during **a** 1980–1998, **b** 1999–2010, and **c** their difference (**b**–**a**). *Positive* means convergence and *negative* means divergence

4.2 Effect of the mean state on anomalous convection response: numerical experiments

In this section, we use two numerical models to verify the abovementioned hypothesis and demonstrate the importance of the mean low-level convergence in determining the location of anomalous convection.

As mentioned above, both SST change and low-level convergence can influence the development of the anomalous convection. However, the magnitude of epochal difference of SST in the EP can only reach −0.3 °C and the mean SST change in the CP is nearly negligible (Fig. 7a). It gives a clue that the direct impact from mean SST change may not be essential in driving the convection difference between CPW and EPW. Hence, the low-level convergence change is the likely cause to determine the westward shift of anomalous convection in the second epoch associated with ENSO.

The above argument is confirmed by the modeling results from the ZC atmospheric model. The first two experiments use the same low-level convergence in the first epoch but SST in two epochs (Fig. 9a, b), and little difference is seen between these two experiments (Fig. 9d). When we use the same SST but different low-level convergence, the resultant surface wind anomalies indeed differ greatly with relative weak westerly anomalies during the second epoch, which tends to generate anomalous reduced convergence in the CP (Fig. 9e). These experiments provide indirect evidence that the anomalous convection prefers to take place in the WP during the second epoch. However, the SST-generated heating in this model is to some extent unrealistic as it is collocated with the prescribed SSTA pattern, so that the westward confinement of heating relative to the SST warming cannot be captured. Moreover, based on the assumption in this model, the heating will remain the same if the mean low-level wind is convergent (Eq. 3), independent of the value of mean low-level convergence. In reality, however, the stronger low-level mean convergence tends to rapidly and effectively transfer the low-level moisture perturbation to the mid-troposphere and generate much stronger mid-tropospheric heating.

To get a more realistic precipitation and heating pattern, we then use the ECHAM (v4.6) atmospheric model with more complete physics to testify the tight relationship between anomalous convection and mean low-level convergence. First, we perform two experiments (CTRL_ID1_old and CTRL_ID2) with prescribed climatological SST during two epochs, i.e., 1980–1998 and 1999–2010 (Table 1), but they both produce strong divergence in the equatorial CP and thus fail to reproduce the observational low-level convergence difference between the two epochs (Fig. 10a, b). Therefore, the resultant anomalous precipitation does not exhibit clear zonal displacement with

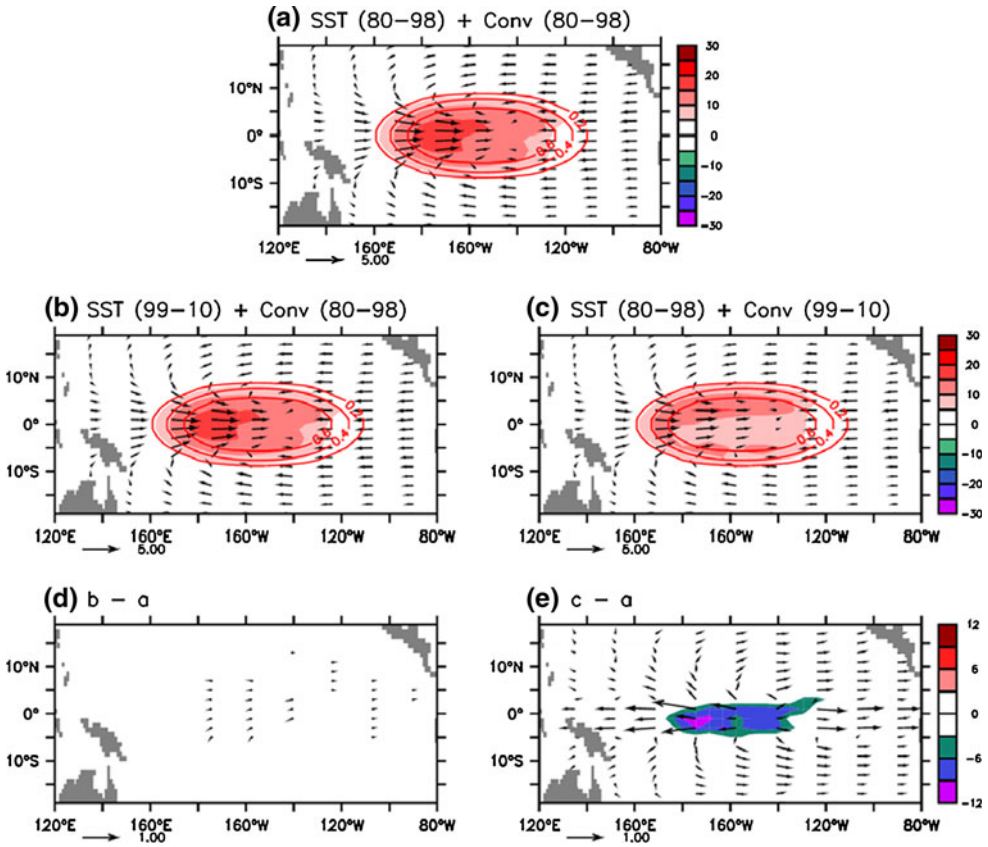

Fig. 9 Atmospheric wind (vectors) response to a prescribed CP SST warming (contours) by using the ZC atmospheric model, with **a** climatological SST during 1980–1998 and low-level convergence during 1980–1998, **b** climatological SST during 1999–2010 and low-level convergence during 1980–1998, **c** climatological SST during 1980–1998 and low-level convergence during 1999–2010. **d** is the difference between **b** and **a**, and **e** is the difference between **c** and **a**. The *shading* denotes the wind convergence ($\times 10^{-7}$ s^{-1})

respect to the same CP SST warming perturbation under the two epochal SST climatologies (not shown).

To reduce mean divergence near the CP, we modify the ECHAM model by imposing a strong nudging to the wind tendency equation, and the nudging is confined to the lowest 4 sigma levels ($16 \leq n \leq 19$) roughly from the 850 hPa to 1,000 hPa. The nudging term is obtained by running an experiment with the wind nudging as

$$\frac{d\bar{u}}{dt}\text{nudging} = [(\bar{u}_c + C_0\delta\bar{u}) - \bar{u}]/8640 \quad (4)$$

where $\bar{u}_c$ is the climatological wind in the control run with climatological SST forcing, $\delta\bar{u}$ is the observed 1,000 hPa wind difference between 1980–1998 and 1999–2010, and $\bar{u}$ is the model simulated wind in each step. C_0 is the coefficient of the wind nudging to allow the imposed wind convergence decrease with the height. Here we use $C_0 = 1$ when $n = 19$ (the lowest level); $C_0 = 0.8$ when $n = 18$; $C_0 = 0.5$ when $n = 17$; $C_0 = 0.2$ when $n = 16$; and $C_0 = 0$ when $n < 16$. We then output this nudging term and add the corresponding climatological nudging term directly to the modified ECHAM model run (CTRL_ID1) in the tropical Pacific east of 180° (Fig. 10d). To make the results more evident in the following sensitivity experiments, the nudging term is amplified so that the simulated epochal difference of the low-level convergence is about twice than the observed (Fig. 10f vs. Fig. 8c). Taking these two experiments (CTRL_ID1 and CTRL_ID2) as the control runs, we add the SST warming in the CP for the sensitivity experiments (SEN_ID1 and SEN_ID2) (Table 1).

For a specified SSTA in CP (Fig. 11a), the ECHAM experiment results show that the precipitation and 1,000 hPa zonal wind response tend to shift westward under the later epochal mean state (SEN_ID2—CTRL_ID2), compared to that under the earlier epochal mean state (SEN_ID1—CTRL_ID1). Interestingly, stronger easterly wind anomalies are seen in the EP with a similar mean state in the second epoch (SEN_ID2-CTRL_ID2) (Fig. 11c). The simulated precipitation and zonal wind phase shift are consistent with those observed, implying that the mean state difference is indeed responsible for the decadal change of the interannual SST-precipitation-zonal wind phase relation. Thus, the weaker mean SST gradient and relatively stronger low-level convergence in CP during the earlier period favor the in-phase anomalous SST-convection relations and thus eastward propagation of the convectively coupled system that eventually form the EPW episode. The stronger mean SST gradient and associated relatively stronger low-level mean divergence in CP during the later period, on the other hand, promotes a westward phase shift of the anomalous

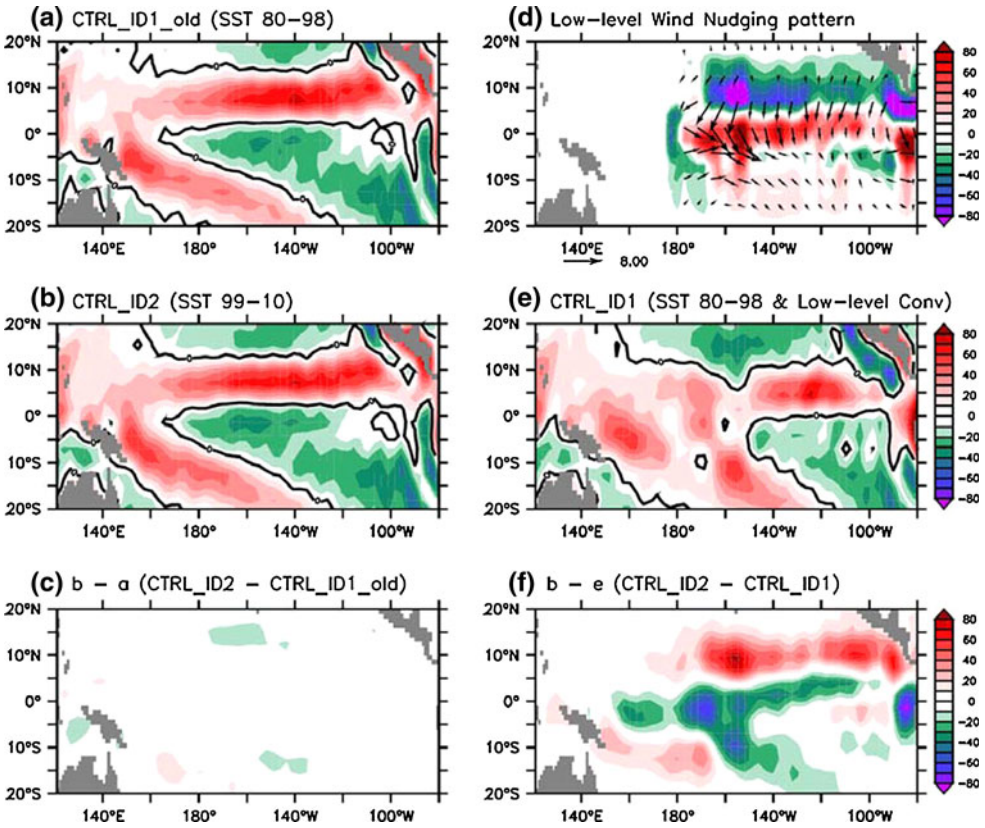

Fig. 10 Low-level (1,000 hPa) wind convergence ($\times 10^{-7}$ s^{-1}) in the ECHAM model with prescribed climatological SST during, **a** 1980–1998 (CTRL_ID1_old), **b** 1999–2010 (CTRL_ID2). **d** is the lowest-level (~1,000 hPa) wind nudging pattern ($\times$1/8640, vectors) and the associated convergence pattern ($\times 10^{-7}$). **e** is the same with **a** but with imposed mean low-level wind convergence in the lowest 4 levels (CTRL_ID1). **c** and **f** are the differences of **b**–**a** and **b**–**e**, respectively

convection, which eventually leads to the development of a CPW.

4.3 Is the epochal mean state change due to the asymmetry of ENSO events?

Considering the short studied period, the mean state change may be partially attributed to the asymmetry of extreme ENSO events (Ashok et al. 2007; Kug et al. 2009; McPhaden et al. 2011). To examine this possibility, we first remove the two extreme El Niño events (1982–1983, 1997–1998), and this La Niña-like mean state change stays robust (Fig. 12a). Further, extreme La Niña events in the second epoch could be another candidate to result in a similar mean state change. Here we adopt 2001-2005 as the second epoch during which there are two El Niño events but without La Niña, the epochal SST difference still exhibits pronounced east–west SST gradient in the equatorial Pacific (Fig. 12b). More importantly, the reduced low-level convergence is apparent for the above two tests (Fig. 12a, b). Actually the low-level convergence in the CP depicts clear decadal shift variability at around 1999 (Fig. 12d), which is dynamically consistent with the enhanced zonal SST gradient between the EP (160°W–120°W, 10°S–10°N) and the WP (120°E–180°, 10°S–10°N) (Fig. 12c). In view of these results, we consider this mean state change to be mainly a reflection of the decadal variability rather than due to the asymmetry of ENSO events.

5 Summary and discussion

After the late 1990s, El Niño events have been observed to occur preferably in the CP with a standing character. We describe this type of El Niño as standing CPW. We offer a new mechanism by ascribing this El Niño property change to a recent mean state characterized by a grand La Niña-like pattern, and more CPW events are anticipated in the coming decades if the La Niña-like pattern persists.

We summarize the major finding into a schematic diagram as shown in Fig. 13. After the late 1990s, this decadal change of the mean state largely suppresses the low-level convergence feedback so that the surface westerly wind anomalies are weakened and shift to the west. At the onset phase (boreal spring), mean low-level divergence in the second epoch tends to shift the anomalous convection and zonal wind response westward, leading to a weak SSTA tendency that is zonally in-phase with the underlying SSTA warming (Fig. 13b). Accompanying the westward-shifted westerly anomalies in the WP are easterly anomalies in the EP (Fig. 13b). This wind pattern readily explains the weak TH, ZA and EK feedbacks in the EP than the CP during boreal spring. In the following summer and autumn, this

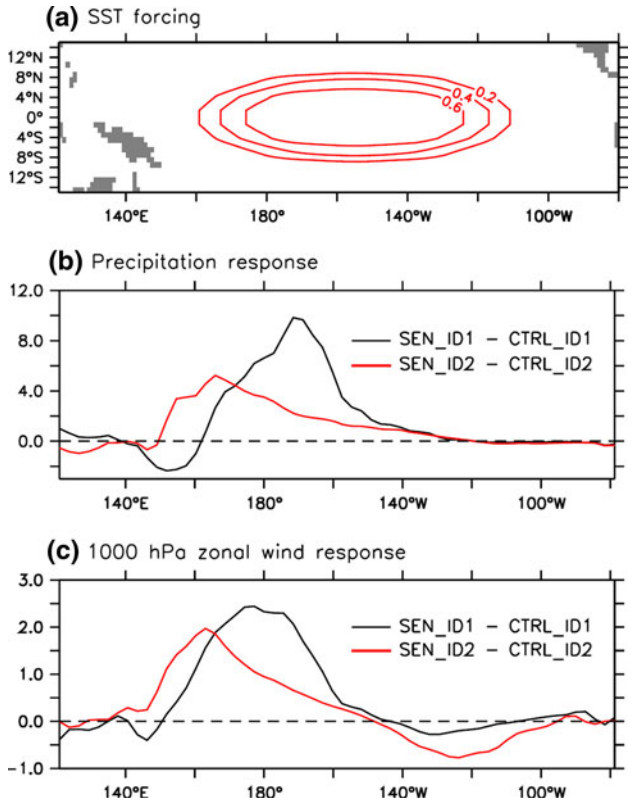

Fig. 11 **a** Prescribed SST warming forcing in the ECHAM model. **b** Anomalous equatorial (5°S–5°N) precipitation (mm/day) response by using the climatological SST during 1999–2010 (*red*, SEN_ID2—CTRL_ID2), and climatological SST during 1980–1998 with imposed mean low-level wind convergence (*black*, SEN_ID1—CTRL_ID1). **c** is the same as **b** but for 1,000 hPa zonal wind anomaly (m/s). Atmospheric precipitation and surface wind are averaged in April–October during which El Niño undergoes intense development

mean state change also displaces the anomalous convection and zonal wind stress anomalies westward to the vicinity of the dateline, facilitating the SSTA to appear in the CP rather than the EP. This differs markedly from the earlier decadal period in which the in-phase convection-SST relation promotes an eastward shift of maximum SSTA tendency due to the integration of the TH and EK feedbacks (Fig. 13a).

Due to less reliable observations, it is difficult to extend the current study to the historical dataset, while this mechanism is confirmed by coupled model results indicating that the CPW prefers to occur in the state with the enhanced mean zonal gradient (La Niña-like pattern), and vice versa (Choi et al. 2011). Choi et al. (2011) emphasized the contributions of ZA feedback associated with enhanced mean SST gradient and air-sea coupling strength in the WP. However, here we underline the role of the suppressed low-level convergence feedback and its strong confinement effect of anomalous convection in the WP. We also agree with Choi et al. (2011) that the possible contribution from global warming cannot be ruled out since it may induce a large CP thermocline uplifting in the future, while the thermocline change is relatively weak in the CP over the recent decades (Fig. 7c).

The westward shift of the convectively coupled system may also directly influence the periodicity of ENSO. The dominant period of the standing CPW during 1999–2010 (1–3 years) is shorter than that of the EPW episodes during 1980–1998 (3–5 years) (Fig. 2e, f). Based on the "delayed" oscillator mechanism (e.g., Suarez and Schopf 1988; Cane et al. 1990), the ENSO period mainly relies on

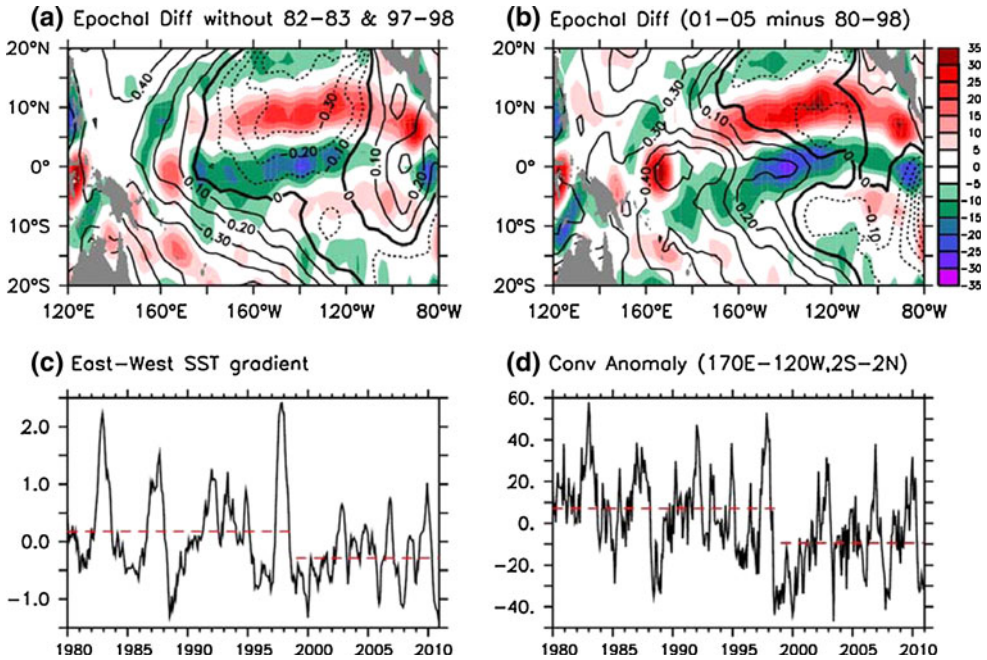

Fig. 12 **a** Epochal SST (contours) and low-level (1,000 hPa) convergence differences without the two strongest EPW (1982–1983 and 1997–1998), **b** The same as a but for epochal difference between 2001–2005 (during which there are no La Niña events) and 1980–1998, **c** The East–West SSTA gradient between the EP (160°W–120°W, 10°S–10°N) and the WP (120°E–180°,10°S–10°N). **d** The CP (170°E–120°W, 2°S–2°N) low-level (1,000 hPa) convergence anomaly. Both the zonal SST gradient and low-level convergence exhibit a strong decadal shift at around 1999 as shown by the *red dashed lines*

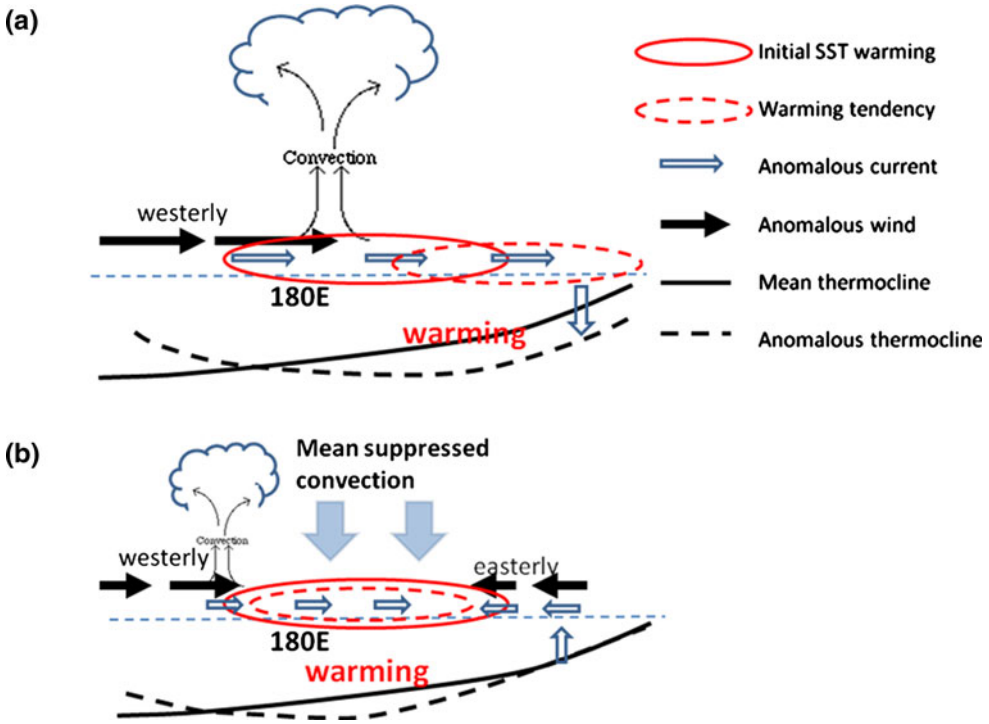

Fig. 13 Schematic diagram describing the major differences between **a** EPW and **b** CPW. In the first epoch (1980–1998), the initial SST warming can drive a strong convection anomaly as well as strong westerly anomalies in the WP, which further cause the eastward displacement of warming tendency because of the zonal and vertical advection. In the second epoch (1999–2010), the La Niña-like mean state (enhanced zonal SST gradient) induces background suppressed convection and low-level divergence over the CP, which tends to reduce the intensity of anomalous convection and shifts it westward due to the *reduced low-level moisture convergence feedback*. The resultant weak westerly (easterly) anomalies in the WP (EP) tend to confine the SST warming tendency in the CP, prompting the generation of CPW

the time of westward propagating Rossby waves. As seen in Fig. 5 of Cane et al. (1990), the westward shifted zonal wind anomaly shortens the distance for the westward propagation of Rossby waves, which shortens the delay and hence shortens the period (An and Wang 2000). Although a longer period will be required for firmer empirical validation, this mechanism is a plausible explanation to the relatively short periodicity of the standing CPW in the recent decade.

Since the La Niña-like mean state change plays an important role in driving the El Niño behavior change in the recent decade, the question arises as to whether this La Niña-like decadal pattern is driven by external anthropogenic forcing or internal natural variability. Previous studies have proposed several different possibilities (Kucharski et al. 2011; Park et al. 2012; Wang et al. 2011). Park et al. (2012) pointed out that it could be triggered by global warming and maintained by the interaction with the North Pacific atmospheric variability. Kucharski et al. (2011) suggested that this La Niña-like pattern can be remotely forced by the basin wide warming in the Atlantic Ocean via changing the Walker circulation, while the Atlantic warming can be a consequence of either anthropogenic forcing or natural multi-decadal variability. Wang et al. (2011) suggested that this La Niña-like pattern can be a manifestation of internal multi-decadal variability. This argument can be supported by two evidences. Firstly, the majority of climate model experiments suggest that increasing greenhouse gas forcing leads to an El Niño-like global warming together with a weakening Walker circulation (e.g., Vecchi and Soden 2007). Secondly, analysis of observed SST for the second half of the 20th century, during which major global warming took place and observations from different independent SST datasets are relatively reliable, yields a consistent El Niño-like global warming (not shown). Here we prefer to regard this epochal mean state change mainly as a natural decadal variability, which is also partially supported by the current climate model that can simulate these two types of Niño without anthropogenic forcing (Yeh et al. 2011). However, more investigation is required to explore the physical mechanism leading to this La Niña-like pattern.

Acknowledgments We would like to thank Dr. Mark A Cane and Jong-Seong Kug for their comments and suggestions on this study. This work has been supported by the Climate Dynamics Program of the National Science Foundation under award No. AGS-1005599, and APEC Climate Center. The authors acknowledge partial support from International Pacific Research Center which is sponsored by the

JAMSTEC, NASA (NNX07AG53G) and NOAA (NA09OAR 4320075). TL is supported by ONR grant N000141210450. This is SOEST contribution number 8690 and IPRC contribution number 895.

References

Adler RF et al (2003) The Version 2 global precipitation climatology project (GPCP) monthly precipitation analysis (1979-present). J Hydrometeor 4:1147–1167

An S-I, Wang B (2000) Interdecadal change of the structure of ENSO mode and its impact on the ENSO frequency. J Clim 13:2044–2055

Ashok K, Behera S, Rao AS, Weng H, Yamagata T (2007) El Niño Modoki and its teleconnection. J Geophys Res 112:C11007. doi:10.1029/2006JC003798

Behringer DW, Xue Y (2004) Evaluation of the global ocean data assimilation system at NCEP: The Pacific Ocean. eighth symposium on integrated observing and assimilation systems for atmosphere, oceans, and land surface, AMS 84th Annual Meeting, Washington State Convention and Trade Center, Seattle, Washington, pp 11–15

Bjerknes J (1969) Atmospheric teleconnections from the equatorial Pacific. Mon Wea Rev 97:163–172

Cane MA, Münnich M, Zebiak SE (1990) A study of self-excited oscillations of the tropical ocean-atmosphere system. Part I: liner analysis. J Atmos Sci 47:1562–1577

Chen G, Tam CY (2010) Different impacts of two kinds of Pacific Ocean warming on tropical cyclone frequency over the western North Pacific. Geophys Res Lett 37:L01803. doi:10.1029/2009GL041708

Choi J, An S-I, Kug J-S, Yeh S-W (2011) The role of mean state on changes in El Niño's flavor. Clim Dyn 37:1205–1215. doi:10.1007/s00382-010-0912-1

Ding Q, Steig EJ, Battisti DS, Küttel M (2011) Winter warming in West Antarctica caused by central Pacific warming. Nat Geosci 4:39–403

Fedorov AV, Philander SGH (2000) Is El Niño changing? Science 288:1997–2002. doi:10.1126/science.288.5473.1997

Ham Y-G, Kug J-S (2011) How well do current climate models simulate two-type of El Niño? Clim Dyn. doi:10.1007/s00382-011-1157-3

Hong C–C, Li Y-H, Li T, Lee M-Y (2011) Impacts of central Pacific and eastern Pacific El Niños on tropical cyclone tracks over the western North Pacific. Geophys Res Lett 38:L16712. doi:10.1029/2011GL048821

Jin F-F, Kim ST, Bejarano L (2006) A coupled stability index for ENSO. Geophys Res Lett 33:L23708. doi:101029/2006GL027221

Kanamitsu M et al (2002) NCEP-DEO AMIP-II Reanalysis (R-2). Bull Amer Met Soc 83:1631–1643

Kao H-Y, Yu J-Y (2009) Contrasting eastern-Pacific and central Pacific types of El Niño. J Clim 22:615–632. doi:10.1175/2008JCLI2309.1

Kim H, Webster P, Curry J (2009) Impact of shifting patterns of Pacific Ocean warming on north Atlantic tropical cyclones. Science 325:77–80

Kucharski F, Kang I-S, Farneti R, Feudale L (2011) Tropical Pacific response to 20th century Atlantic warming. Geophys Res Lett 38:L03702. doi:10.1029/2010GL046248

Kug J-S, Jin F–F, An SA (2009) Two types of El Niño events: cold tongue El Niño and warm pool El Niño. J Clim 22:1499–1515. doi:10.1175/2008JCLI2624.1

Kumar KK, Rajagopalan B, Hoerling M, Bates G, Cane M (2006) Unraveling the mystery of Indian Monsoon failure during El Niño. Science 314:115–119

Larkin NK, Harrison DE (2005) Global seasonal temperature and precipitation anomaly during El Niño autumn and winter. Geophys Res Lett 32:L16705. doi:10.1029/2005GL022860

Lee T, McPhaden MJ (2010) Increasing intensity of El Niño in the central-equatorial Pacific. Geophys Res Lett 37:L14603. doi:10.1029/2010GL044007

Li T (1997) Phase transition of the El Niño-Southern Oscillation: a stationary SST mode. J Atmos Sci 54:2872–2887

Li T, Hogan TF (1999) The role of the annual mean climate on seasonal and interannual variability of the tropical Pacific in a coupled GCM. J Clim 12:780–792

Lorenzo Di et al (2010) Central Pacific El Niño and decadal climate change in the North Pacific Ocean. Nat Geosci 3:762–765

McPhaden MJ, Lee T, McClurg D (2011) El Niño and its relationship to changing background conditions in the tropical Pacific Ocean. Geophys Res Lett 38:L15709. doi:10.1029/2011GL048275

Park J-S, Yeh S-W, Kug J-S (2012) Revisited relationship between tropical and North Pacific sea surface temperature variations. Geophys Res Lett 39:L02703. doi:10.1029/2011GL050005

Roeckner E (1996) The atmospheric general circulation model ECHAM-4: model description and simulation of present-day climate. Max-Planck-Institute Meteorol Rep 218:90

Smith TM, Reynolds RW, Peterson TC, Lawrimore J (2008) Improvements to NOAA's Historical Merged Land-Ocean Surface Temperature Analysis (1880–2006). J Clim 21:2283–2293

Solomon S et al (2010) Contributions of stratospheric water vapor to decadal changes in the rate of global warming. Science 327:1219–1223

Su J, Zhang R, Li T, Rong X, Kug J-S, Hong C–C (2010) Amplitude asymmetry of El Niño and La Niña in the eastern equatorial Pacific. J Clim 23(3):605–617

Suarez MJ, Schopf PS (1988) A delayed action oscillator for ENSO. J Atmos Sci 45:3283–3287

Vecchi GA, Soden BJ (2007) Global warming and the weakening of the tropical circulation. J Clim 20:4316–4340

Wang B (1995) Interdecadal changes in El Niño onset in the last four decades. J Clim 8:258–267

Wang B, Liu J, Kim H-J, Webster PJ, Yim S-Y (2011) Recent change of global monsoon precipitation (1979–2008). Clim Dyn. doi:10.1007/s00382-011-1266-z

Weng H, Ashok K, Behera WK, Rao SA, Yamagata T (2007) Impacts of recent El Niño Modoki on dry/wet conditions in the Pacific rim during boreal summer. Clim Dyn 29:113–129

Weng H, Behera S, Yamagata T (2009) Anomalous winter climate conditions in the Pacific Rim during recent El Niño Modoki and El Niño events. Clim Dyn 32:663–674. doi:10.1007/s00382-008-0394-6

Xiang B, Wang B, Ding Q, Jin F–F, Fu X, Kim H-J (2011) Reduction of the thermocline feedback associated with mean SST bias in ENSO simulation. Clim Dyn. doi:10.1007/s00382-011-1164-4

Yeh S-W, Kug J-S, Dewitte B, Kwon M-H, Kirtman B, Jin F–F (2009) El Niño in a changing climate. Nature 461:511–514. doi:10.1038/nature08316

Yeh S-W, Kirtman BP, Kug J-S, Park W, Latif M (2011) Natural variability of the central Pacific El Niño event on multi-centennial timescales. Geophys Res Lett 38:L02704. doi:10.1029/2010GL045886

Yu J-Y, Kao H-Y, Lee T (2010) Subtropics-related interannual sea surface temperature variability in the central equatorial Pacific. J Clim 23:2869–2884

Zebiak SE (1986) Atmospheric convergence feedback in a simple model for El Niño. Mon Wea Rev 114:1263–1271

Zebiak SE, Cane MA (1987) A Model El-Niño Southern Oscillation. Mon Wea Rev 115:2262–2278